JOURNAL OF SPACECRAFT AND ROCKETS
Vol. 36, No. 5, September–October 1999

Development of Pulsed Arc Heater for Small Hypersonic High-Enthalpy Wind Tunnel

Leonardo Biagioni* and Fabrizio Scortecci†
Centrospazio–CPR, I-56014 Ospedaletto, Italy
and
Fabrizio Paganucci‡
University of Pisa, I-56100 Pisa, Italy

A pulsed arc heater was designed, manufactured, and installed in Centrospazio laboratory to equip a newly developed hypersonic, high-enthalpy, small-scale blowdown wind tunnel. The facility operates with air in the low to medium Reynolds number range (10^4–10^6) and is capable of producing Mach 6 airflows, with a specific total enthalpy up to 3 MJ/kg, on a 60-mm effective diameter test section. The heater is run in a pulsed, quasisteady mode, with test time ranging between 10 and 50 ms. The flow is directly heated by the electric arc established between two coaxial electrodes, powered by a large capacitor bank. A suitable plenum chamber placed just downstream of the discharge chamber allows the flow to reach thermochemical equilibrium before the expansion in the wind-tunnel nozzle and enhances mixing, thereby reducing radial gradients. A numerical model was developed to simulate the unsteady gasdynamic behavior of the arc heater and was used during the design phase to optimize the geometric and temporal parameters of the heater and to assess the hypersonic tunnel useful test time. Experimental results compare favorably with numerical predictions, with the plenum pressure history matching within 5% and plenum temperature within 10%. More than 600 runs have been performed so far, demonstrating the heater reliability and capabilities.

Nomenclature

A	= restricted section area, m^2
C_p	= gas constant pressure specific heat, $J \cdot kg^{-1} \cdot K^{-1}$
C_v	= gas constant volume specific heat, $J \cdot kg^{-1} \cdot K^{-1}$
C_0	= arc characteristic constant, $V \cdot A^k \cdot m^{-1} \cdot Pa^m$
I	= arc current, A
k	= arc characteristic coefficient
M	= restricted section Mach number
m	= arc characteristic coefficient
$\dot{m}$	= mass flow rate, $kg \cdot s^{-1}$
p	= static pressure, Pa
R	= gas constant, $J \cdot kg^{-1} \cdot K^{-1}$
T	= static temperature, K
t	= time, s
V	= chamber volume, m^3
v	= flow velocity, $m \cdot s^{-1}$
W_{th}	= thermal input power, W
Γ	= internal energy function, $J \cdot K^{-1}$
γ	= gas specific heat ratio
Δh	= enthalpy variation, $J \cdot kg^{-1}$
ΔV	= voltage difference, V
Δx	= electrodes distance, m
ε	= arc efficiency
η	= restricted section discharge coefficient

Subscripts

electrodes	= electrode conditions
in	= incoming flow
out	= outgoing flow
restr	= restricted section
sheaths	= electrode sheath conditions
tot	= stagnation conditions
0	= initial conditions

Presented as Paper 97-3016 at the AIAA/ASME/SAE/ASEE 33rd Joint Propulsion Conference, Seattle, WA, 6–9 July 1997; received 11 February 1999; revision received 7 May 1999; accepted for publication 18 May 1999.

*Graduate Student, Via Gherardesca 5. Student Member AIAA.
†Senior Research Engineer, Via Gherardesca 5. Member AIAA.
‡Assistant Professor, Department of Aerospace Engineering, Via Diotisalvi 2. Member AIAA.

Introduction

A SMALL hypersonic high-enthalpy, arc-heated, blowdown wind tunnel (HEAT) was recently developed and installed in Centrospazio laboratory,[1] to perform experiments in the framework of the ESA Future European Space Transportation Investigation Program (FESTIP).[2] The tunnel is capable of delivering Mach 6 airflows (Mach 8.5 runs in helium have also been performed) with a specific total enthalpy up to 3 MJ/kg, on an effective test section with a 60 mm diam, in the low to medium Reynolds number range (10^4–10^6). The facility operates in a pulsed, quasisteady mode, with running time ranging between 10 and 50 ms, therefore allowing for a simple, uncooled design to be feasible and effective.[3]

The HEAT facility mainly consists of an arc-driven gas heater and a contoured expansion nozzle[4] exhausting in a dump tank with a 4.1 m^3 volume. Auxiliary systems are fitted to the arc heater to provide it with working fluid and energy, as will be described. The tank is evacuated by four rotary pumps until a pressure of 10 Pa is reached. This pressure level allows an underexpanded hypersonic jet to be maintained at the nozzle exit for a running time in excess of 200 ms. However, the presently available power system limits the steady-state hot pulse to less than 50 ms.

The present work deals with the arc heater design and the experimental characterization carried out so far, using air as the working fluid. Measurements of arc input power, stagnation temperature, and pressure in the plenum chamber during the power pulse are illustrated.

Arc Heater Description

The arc heater consists of two electrodes positioned in a discharge chamber and a suitable plenum/mixing chamber. The cathode is machined out of a 2%-thoriated tungsten rod, measuring 10 mm in diameter; a boron nitride constricted channel (constrictor) separates the cathode from the annular coaxial copper anode. The test fluid (air in the present case) is injected into the discharge chamber through two fast acting solenoid valves and is heated by the electric arc sparking between the electrodes. The constrictor provides

arc stability and improves thermal energy exchange between the arc column and the surrounding flow. A coaxial magnetic field (with intensity of a few tenths of gauss) is applied in the discharge region to spin the arc and, therefore, avoid its concentration on a single anode spot.[5] Two boron nitride perforated screens are placed just downstream of the anode, both to collect particles sputtered from the electrodes and to enhance turbulence in the plenum chamber, because turbulent mixing promotes a more uniform radial distribution of enthalpy across the stream.

The arc heater was designed in a highly modular and operationally flexible way, to be easily modified for different test campaigns. Different electrode arrangements and constrictor configurations can be easily installed, and insulating spacers of different length can be mounted to increase the plenum chamber volume if necessary. A view of the heater is shown in Fig. 1.

The plenum chamber is designed to give the flow a sufficiently long residence time in the high-pressure region, to reach chemical and thermodynamic equilibrium before the expansion in the wind-tunnel nozzle. Although plenum conditions are in full thermochemical equilibrium, this is not the case for the flow in the test section: A significant portion (up to 20%) of the specific enthalpy is frozen in nonequilibrium vibrational modes during the sudden nozzle expansion. This problem is well known to the experimental practitioner and is almost unavoidable in small, hypersonic, high-enthalpy wind tunnels operating with air. Nevertheless, the nonequilibrium expansion of a gas through a hypersonic nozzle is a well understood and widely studied problem since the early 1960s,[6] and frozen test section conditions can be properly assessed as long as the fluid is fully in equilibrium upstream of the nozzle. To this purpose, a computer program was developed to study the nonequilibrium evolution of air flowing through the plenum chamber. A six-reactions chemical model was used,[7] whereas the Landau–Teller model was assumed for vibrational relaxation, with constants obtained from the available literature.[8,9] The results obtained show that complete relaxation from the arc column conditions, that is, fully dissociated, partly ionized, is achieved over a distance of a few millimeters for plenum conditions of a few bars in pressure and less than 3000 K in temperature. Clearly, these results represent only an order of magnitude estimate; nevertheless, they seem appropriate for a conservative design of the plenum chamber, provided its length is much longer than the evaluated relaxation length.

The gas feeding system was designed to supply smooth and repeatable cold-flow pulses with duration of about 100 ms. The air pulse is produced by opening two fast acting solenoid valves. Each valve is activated by a rectangular electric signal generated by a programmable electronic board. A 0.005-m^3 reservoir is placed just upstream of each valve to maintain a quasiconstant back pressure during the pulse. In this way, a steady-state flow is reached a few milliseconds after the valve activation. Both the mass flow rate and the gas pulse duration can be easily adjusted by setting, respectively, the reservoir pressure (up to 50 bar) and the electric pulse duration.

The electrical power system consists of a 12.5 mF main capacitor bank (MCB), which can be charged up to 2400 V, storing a total energy of 36 kJ (Fig. 2). A resistor–inductor matching network is wired between the capacitor bank and the arc heater, to obtain a discharge current time evolution with a roughly constant plateau of duration not shorter than 15 ms, during which a power up to 200 kW is supplied to the electrodes. A high-voltage ignitron device is used to command the arc ignition at the desired moment (programmable with a resolution of 0.5 ms) to maximize the useful run time. The initial MCB voltage is not sufficient to obtain a direct electric breakdown through air at the nominal pressure level. Therefore, an additional network consisting of a 600-μF igniting capacitor bank (ICB) and a 20-mH inductance is permanently connected in parallel with the main power unit. This network is used to self-ignite the discharge as soon as air begins to flow across the electrodes and the pressure reaches a critical value in accordance with Paschen law[10] (typically in the order of a few hundred pascal). The discharge self-ignition takes place a few milliseconds after the

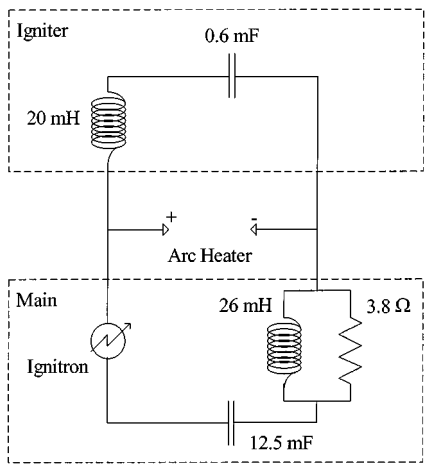

Fig. 2 Electric feeding system schematic.

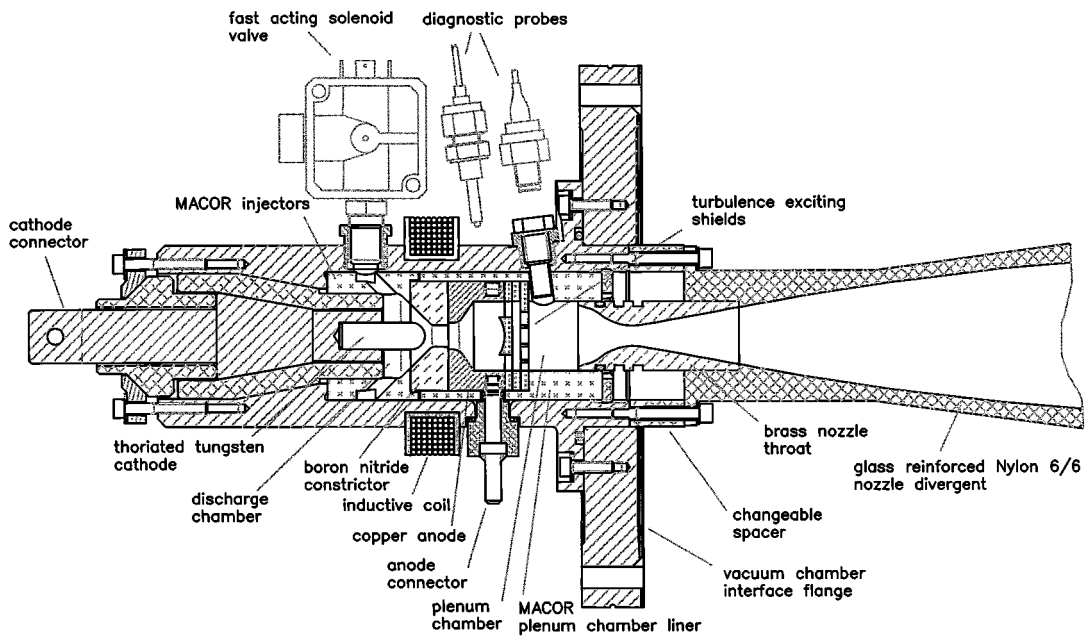

Fig. 1 Arc heater.

valve opening: the ICB is rated to sustain 30–40 A of discharge current for a few milliseconds, that is, until the discharge chamber pressure reaches the desired value (of about 2 bar) and the ignitron is switched on, allowing the MCB to supply energy to the arc. This arrangement allows for energizing the gas when a significant ionization (produced by the ICB discharge) is already present, thus facilitating the high-pressure breakdown and establishing a stable MCB-driven arc, with duration and characteristic determined by the overall network scheme.

Arc Heater Numerical Simulations

To optimize the arc heater geometry on the basis of the gasdynamic system behavior, a numerical model based on a lumped-parameter/control-volume approach was developed and implemented in a suitable computer code. The facility is schematized as composed by a series of volumes (capacitive elements) connected through restricted sections (resistive elements).

The volume elements are modeled assuming space-independent gasdynamic parameters (equal to an equivalent average value), the working fluid is considered to be a thermally perfect gas, and conduction and radiation effects are neglected. Finally, the kinetic energy contribution to the total enthalpy is neglected (equivalent to assuming subsonic flow). Accordingly, the Eulerian unsteady conservation equations for the flow are integrated over the volume. For each volume element, a set of two coupled time-dependent integral equations is obtained, one for the pressure derivative and the other for the temperature derivative. The equations are written in general form as

$$\dot{p} = \left[\left(\sum_i \dot{m}_{\text{in}_i} - \sum_j \dot{m}_{\text{out}_j}\right)\right]\frac{RT}{V} + \frac{\dot{T}\left[p_0 + \int_0^t \dot{p}(t')\,\mathrm{d}t'\right]}{T} \tag{1}$$

$$\dot{T} = \frac{\sum_i \left\{\dot{m}_{\text{in}_i}\left[C_p T_{\text{in}_i} + \left(v_{\text{in}_i}^2/2\right)\right]\right\}}{\Gamma} - \frac{\sum_j \left\{\dot{m}_{\text{out}_j}\left[C_p T + \left(v_{\text{out}_j}^2/2\right)\right]\right\}}{\Gamma} - \frac{\left(\sum_i \dot{m}_{\text{in}_i} - \sum_j \dot{m}_{\text{out}_j}\right)C_v T}{\Gamma} + \frac{W_{\text{th}}}{\Gamma} \tag{2}$$

where

$$\Gamma = C_v \frac{p_0 V}{RT_0} + C_v \int_0^t \left[\sum_i \dot{m}_{\text{in}_i}(t') - \sum_j \dot{m}_{\text{out}_j}(t')\right]\mathrm{d}t' \tag{3}$$

The interface conditions between volume elements, that is, the restricted section elements, are modeled using quasi-one-dimensional steady gasdynamic relations, obtaining a set of three algebraic equations as follows:

$$\dot{m} = \sqrt{\eta}\frac{p_i A_{\text{restr}}}{\sqrt{T_{\text{tot}_i}}} \cdot M_{\text{restr}} \cdot \sqrt{\frac{\gamma}{R}\left(1 + \frac{\gamma - 1}{2}M_{\text{restr}}^2\right)^{(1+\gamma)/(1-\gamma)}} \tag{4}$$

$$M_{\text{restr}} = \sqrt{\min\left\{1, [2/(\gamma - 1)] \cdot \left[(p_{\text{in}}/p_{\text{out}})^{(\gamma-1)/\gamma} - 1\right]\right\}} \tag{5}$$

$$T_{\text{tot out}} = T_{\text{tot in}} + [W_{\text{th}}/(\dot{m} \cdot C_p)] \tag{6}$$

For simplicity, the possible development of standing shocks inside the arc heater is neglected. This assumption is not satisfied during the very first moments following the valves opening. Nevertheless, it seems reasonable to believe that such initial phenomena do not affect the subsequent behavior of the system.

Schematizing the heater as composed of four volumes connected by three sections (as shown in Fig. 3), the resulting dynamic system is described by a set of 17 coupled equations. The forcing actions on the system are the solenoid valves opening (described by a trapezoidal law) and the power input from the arc column to the gas. Two different power input laws were examined for the present work: a simplified trapezoidal input and a real input signal as directly measured at the electrodes. The former case was considered during the preliminary design phase, during which the detailed arc behavior was still unknown; the latter was considered for model validation, by comparing numerical and experimental results.

The optimal arc heater configuration was investigated by varying the geometrical parameters, some of which are constrained by dimensional and/or operational limits. Specifically, the reservoir volume and pressure cannot exceed, respectively, 0.01 m^3 and 50 bar, for assembly and safety reasons; the injector effective area must be a multiple of 12.5 mm^2 to allow the adoption of available, commercial valves; the plenum chamber volume cannot be less than 25 cm^3 to permit installation of ceramic screens; the length cannot be less than 15 mm to allow for full chemical and vibrational relaxation of the flow (three times the relaxation length as computed by the earlier described model); and the nozzle throat area is dictated by the Mach 6 condition in the 60-mm-diam test section.

The optimization objective was to maximize the time length of the quasisteady hot-gas pulse, for a given discharge time. Steadiness conditions were evaluated in terms of stagnation pressure and temperature inside the plenum chamber, which, in good approximation, also represent the stagnation conditions in the hypersonic test section. Optimization was performed referring to a nominal test condition, shown in Table 1. A second condition was subsequently verified (Table 2) to assess operational flexibility of the facility.

The preceding set of integral–differential equations was solved numerically, by means of an Adams–Gear–Gauss algorithm, with variable step size and error control. The numerical accuracy of the algorithm was set as follows: maximum relative error 10^{-3} (that is, accuracy within 0.1%), maximum absolute error 10^{-6}, and minimum step size 10^{-6} s. The optimal volume for both the discharge and plenum chambers was found to be slightly larger than the minimum allowed. The optimal time delay for the MCB ignition was found

Table 1 First test condition (nominal)

Variable	Value	Unit
Mach number	6	
Unit Reynolds number	0.8×10^6	m^{-1}
Specific enthalpy	2.0	$MJ \cdot kg^{-1}$
Stagnation temperature	1800	K
Stagnation pressure	590	kPa

Table 2 Second test condition (additional)

Variable	Value	Unit
Mach number	6	
Unit Reynolds number	0.8×10^6	m^{-1}
Specific enthalpy	1.1	$MJ \cdot kg^{-1}$
Stagnation temperature	1080	K
Stagnation pressure	300	kPa

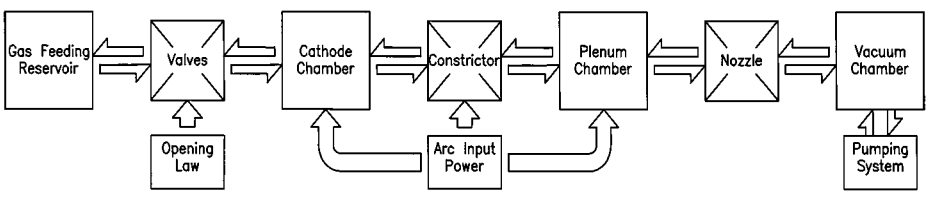

Fig. 3 Arc heater lumped-parameter model.

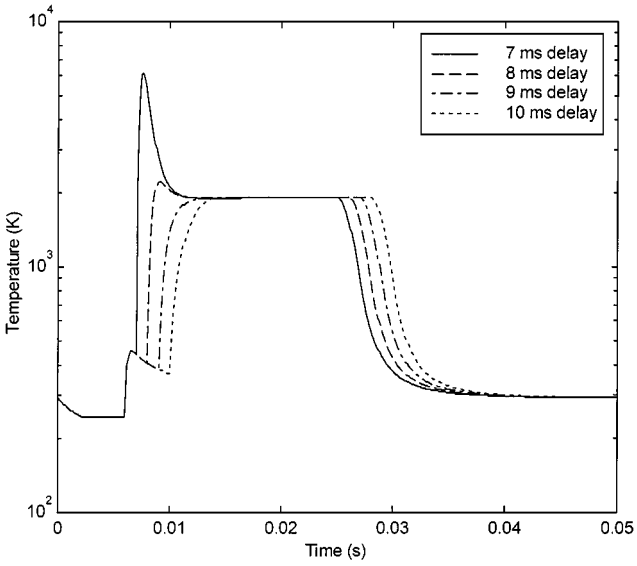

Fig. 4 Ignition delay effect on computed plenum temperature history.

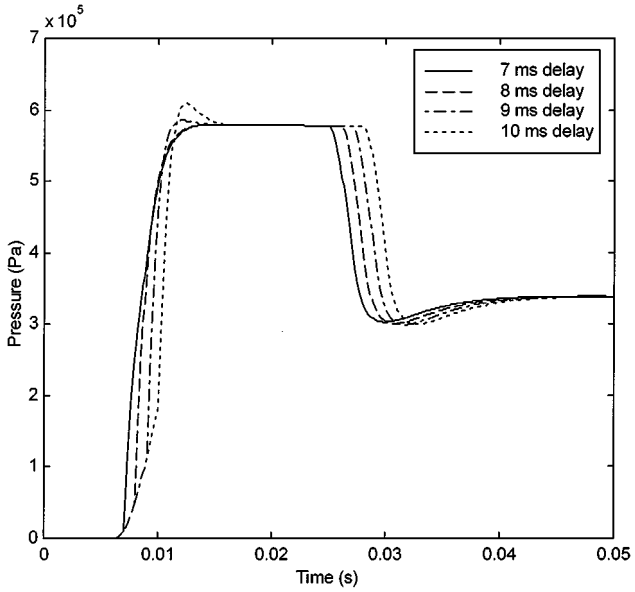

Fig. 5 Ignition delay effect on computed plenum pressure history.

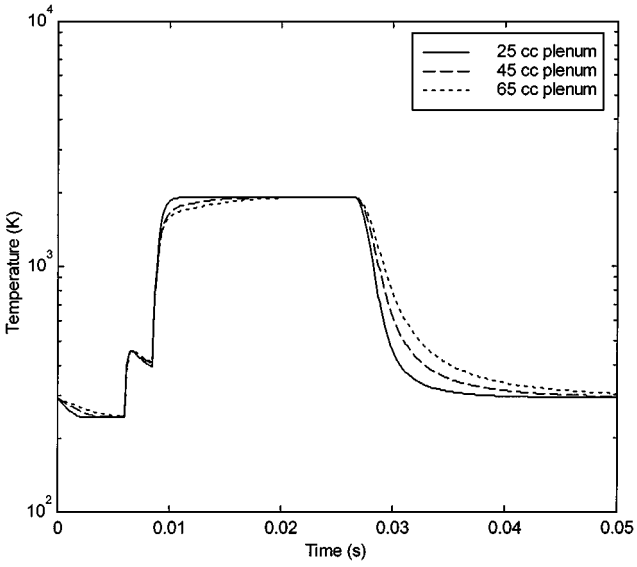

Fig. 6 Plenum volume effect on computed plenum temperature history.

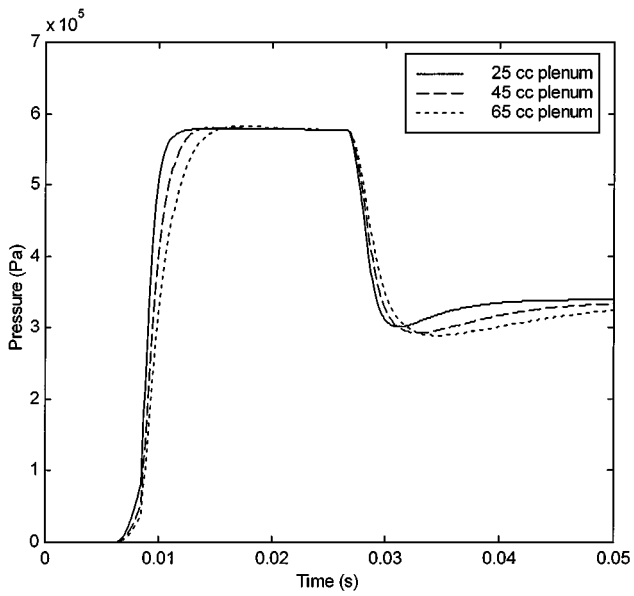

Fig. 7 Plenum volume effect on computed plenum pressure history.

to be approximately 8–9 ms, depending on the test conditions. A reservoir pressure of 710 kPa and 48 kW of input power are needed to generate the flow conditions shown in Table 1.

Parametric plots are shown in Figs. 4–7, together with a full set of results for the optimal configuration at the design test conditions (Figs. 8–11). It can be seen that the mass flow rate keeps constant (and equal to 0.024 kg/s) through the arc heater during the MCB discharge, showing that steady conditions are indeed reached. Flow is subsonic everywhere inside the heater (therefore, justifying the no-shocks assumption) and only the nozzle throat is sonic.

Tuning of the simulation parameters, that is, restricted sections efficiencies, was performed by fitting computed results to measured data for a series of cold runs, during which a gas pulse was generated with no arc discharge. Good agreement was obtained, showing that the numerical model can correctly describe at least the cold-flow case. In Fig. 12 a comparison between the numerically calculated and experimentally measured stagnation pressure in the plenum chamber is shown, for a cold run with a reservoir pressure of 690 kPa.

Experimental Characterization

An experimental program was conducted to assess the capabilities of the arc heater. Measurements of stagnation pressure and temperature in the plenum chamber and voltage and current (and, therefore, power) at the electrodes were carried out using synthetic air as the working fluid. The plenum pressure was measured using a fast response, ruggedized silicon diaphragm transducer (nominal uncertainty 0.1% of full-scale output, ±1.7 kPa); the temperature was measured using unshielded platinum/platinum-rhodium thermocouples, 0.025 mm in diameter (maximum uncertainty ±3.7 K, American Society for Testing and Materials standard). The current flowing through the electrodes was measured by means of a Hall-effect probe (nominal uncertainty 1% of full-scale output, ±2 A), whereas the arc voltage drop was measured using suitable high-voltage probes (relative uncertainty 0.001%, maximum ±1.5 V), the electrodes being floating with respect to the ground. A digital transient recorder controlled by a personal computer and a 12-bit analog-to-digital converting board installed in a workstation were used for data acquisition, storage, and analysis. Because the thermocouple response time is not sufficient to properly resolve the arc running time, a numerical correction method[11,12] was employed to calculate instantaneous temperatures from thermocouple measurements. The combined uncertainty due to the numerical correction was ±45 K.

Figures 13 and 14 show the time history of the main electric and gasdynamic arc heater parameters during a typical run, with the time axis origin corresponding to the valve opening. In Fig. 13,

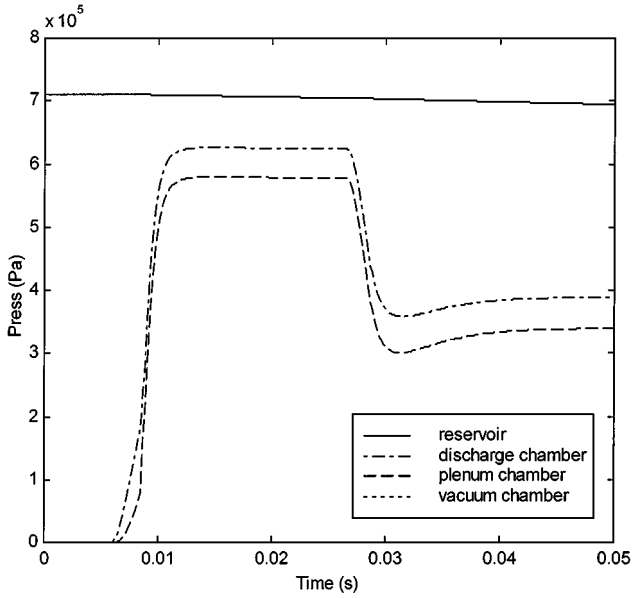

Fig. 8 Computed pressure histories (optimal configuration).

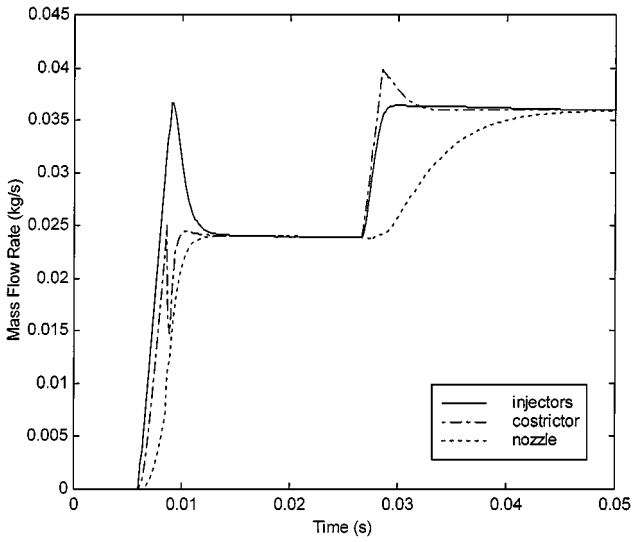

Fig. 9 Computed mass flow rate histories (optimal configuration).

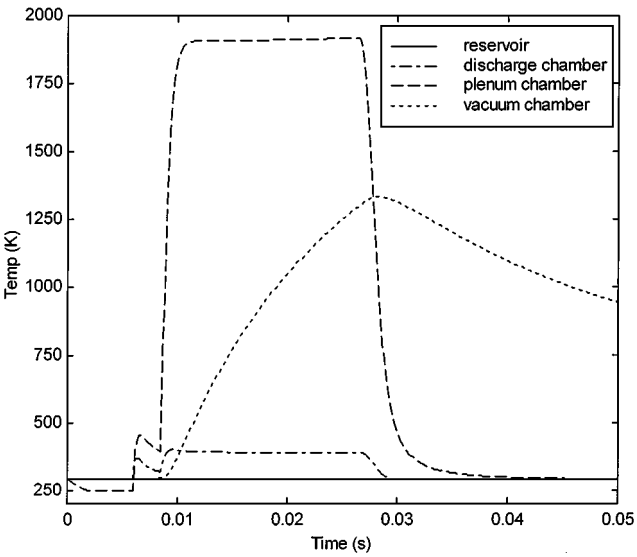

Fig. 10 Computed temperature histories (optimal configuration).

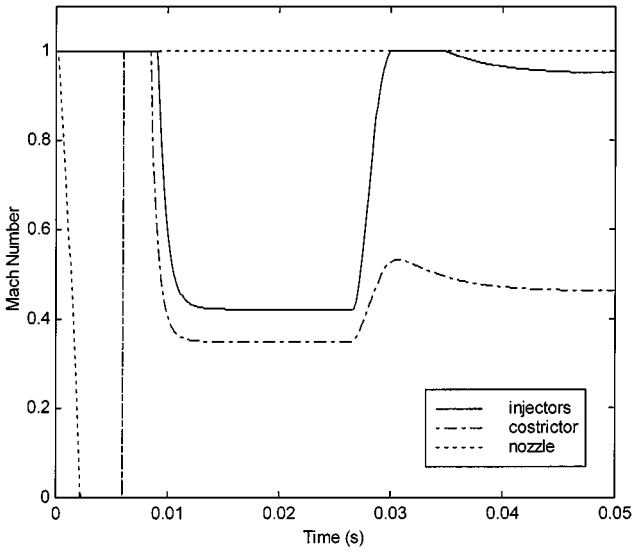

Fig. 11 Computed Mach number histories (optimal configuration).

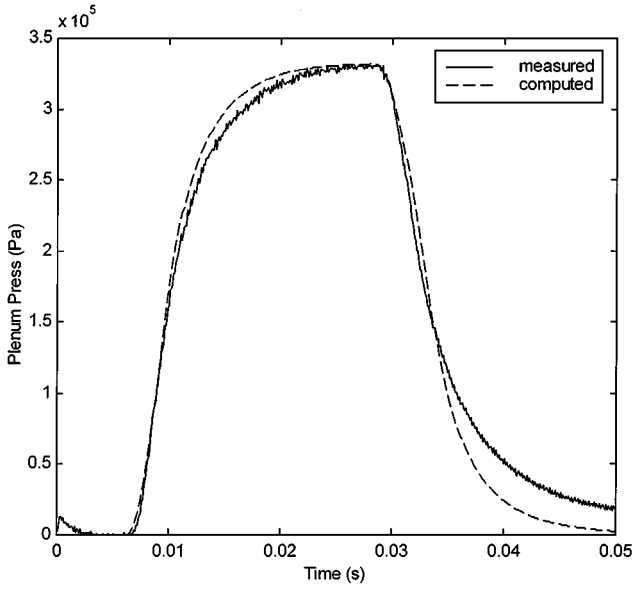

Fig. 12 Measured and computed plenum pressure histories (cold run).

the arc power measured at the electrodes is shown, and the self-ignited current produced by the ICB additional network can be seen, together with the steep current increase (produced by the MCB network) occurring when the ignitron is activated, 9 ms after the valve opening. Figure 14 shows the pressure measured in the plenum chamber. The pressure rise induced by the electric discharge heat input is clearly visible.

A series of runs was performed to assess the steadiness and repeatability of the arc heater performance, for the two operation conditions considered. During these runs the main heater controlling parameters, that is, reservoir pressure and MCB voltage charge, were kept constant. Higher enthalpy runs (Table 1) were performed with a reservoir pressure of 900 kPa and a MCB voltage of 1220 V, whereas lower enthalpy runs (Table 2) were performed with a reservoir pressure of 500 kPa and a MCB voltage of 735 V. Sample results for a 10-ms time interval during the quasisteady phase are shown in Figs. 15–17. The measured data indicate that fair repeatability exists both for pressure and temperature in the plenum chamber.

Tests were also performed at higher energy levels to assess the heater reliability for conditions closer to the operating limit. Though a proper characterization could not be performed, stagnation temperatures and pressures up to 2800 K and 1 MPa, respectively, were obtained by charging the MCB up to 1800 V.

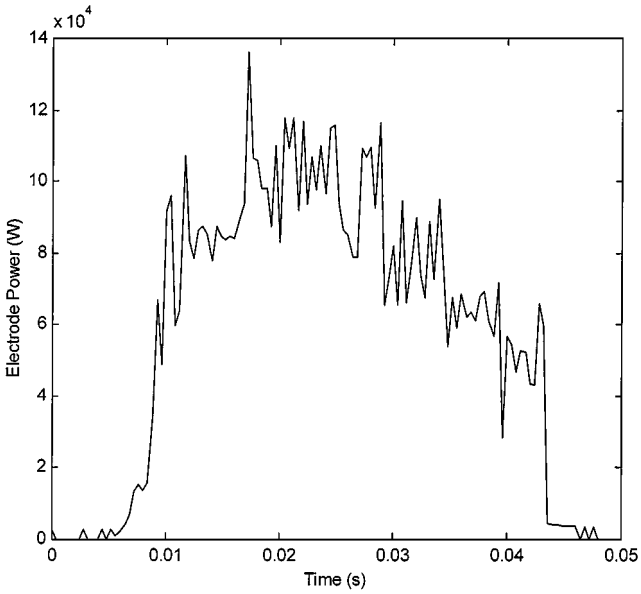

Fig. 13 Measured electrodes power input history (run d3008-4).

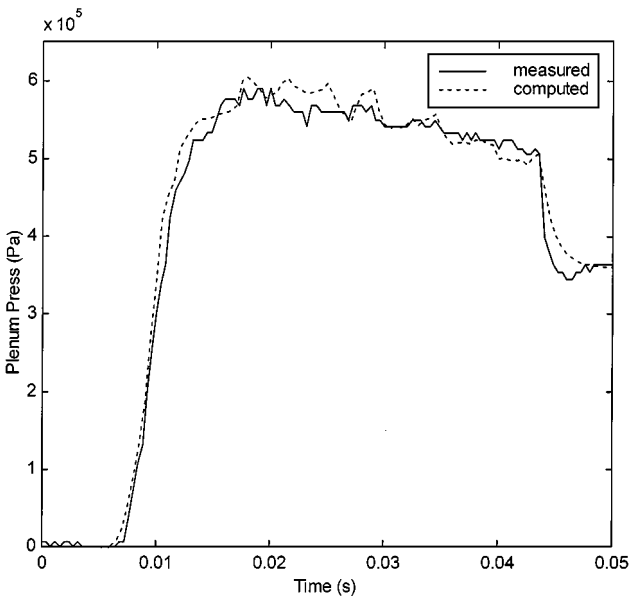

Fig. 14 Measured and computed plenum pressure histories (run d3008-4).

The simulation code was validated against experimental data by using actual measured power signals as inputs for the program. An energy transfer efficiency ε was introduced to take into account heat losses (due to conduction and radiation) and electrode sheath losses. Efficiency was, therefore, defined as

$$\varepsilon = \frac{\dot{m} \cdot \Delta h_{\text{flow}}}{I \cdot \Delta V_{\text{electrodes}}} \tag{7}$$

which in turn can be expanded in the product of a term relevant to electrode sheath losses and a term relevant to thermal losses,

$$\varepsilon = \varepsilon_{\text{thermal}} \cdot \varepsilon_{\text{electrodes}} \tag{8}$$

For short-run duration, during which the average facility wall temperature is not significantly increasing, the thermal efficiency can be assumed as constant (and roughly equal to 0.6 for the present case[13]). However, from classical electric arc theory,[14,15] an analytical expression can be obtained for the electrodic efficiency, therefore, yielding the following relation for the total efficiency:

$$\varepsilon = 0.6 \cdot \left[1 - \frac{V_{\text{sheaths}}}{\Delta V_{\text{electrodes}}}\right] \tag{9}$$

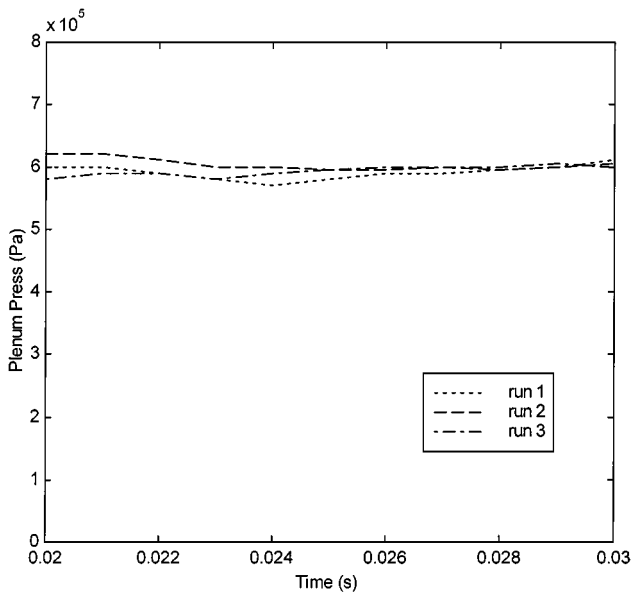

Fig. 15 Plenum pressure repeatability (higher enthalpy).

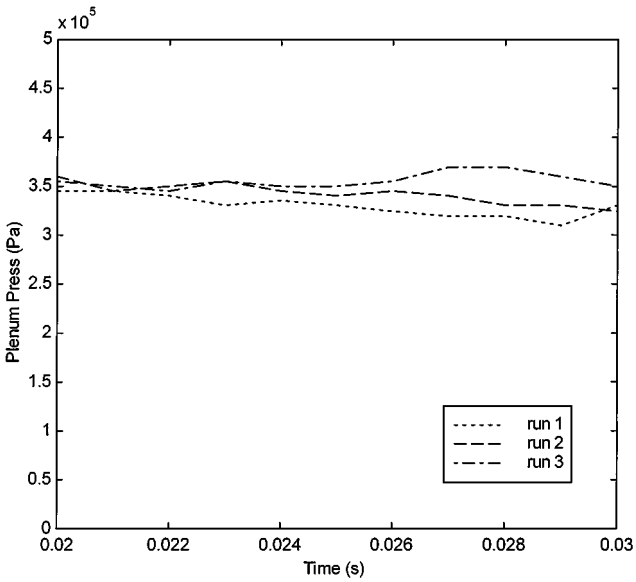

Fig. 16 Plenum pressure repeatability (lower enthalpy).

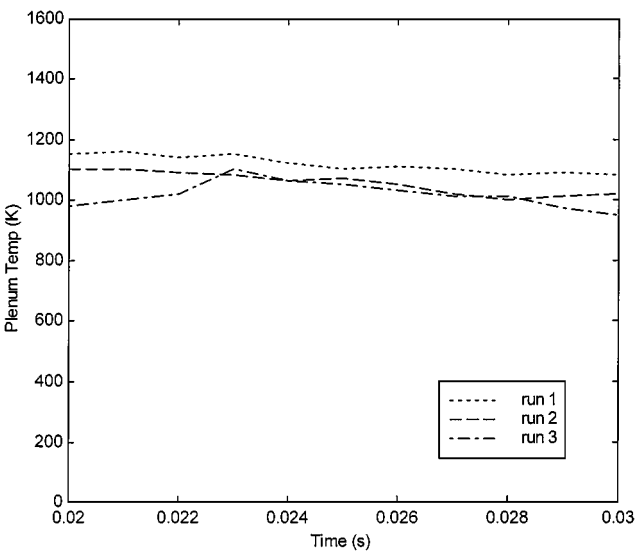

Fig. 17 Plenum temperature repeatability (lower enthalpy).

$$\Delta V_{\text{electrodes}} = \Delta x \cdot C_0(p^m / I^k) \tag{10}$$

where V_{sheaths} is the sum of cathode and anode sheath voltage fall, amounting to about 35 V in the present case. The arc characteristic constants for air were empirically found to be $m = 0.31$ and $k = 0.60$ (Ref. 14).

Good agreement between experimental and numerical results was found for every case considered, with total efficiency values ranging between 0.3 and 0.5, depending on the arc power input. An example is shown in Fig. 14, in which the experimentally measured plenum pressure time history is compared to numerical results (computed using the actually measured electrode power time history as input). It can be seen that an actual power signal is quite different from the ideal trapezoidal one assumed during the preliminary computations, nevertheless, pressure seems to be scarcely affected by the large oscillations in the power signal but appear dependent on the average value only. Within the explored operational range, it appears that the numerical model can provide a good estimate of the arc heater characteristics, proving to be a valuable tool to quickly verify the feasibility of different test conditions.[16]

The main problem evidenced during the heater operation was the occasional occurrence of anomalous discharge modes characterized by extremely high current intensities that were the major source of component deterioration.[3] In the final design, anomalous discharges have been effectively controlled, though not completely eliminated, using a constricted discharge chamber and spinning the arc by means of a coaxial magnetic field.[5]

Even for proper operation, some level of electrode degradation cannot be avoided. As usually occurring with pulsed arc devices, repeated starts cause significant electrode erosion, which in the case of HEAT arc heater is enhanced by the relatively high discharge pressure and the low electrode wall temperature. On cold electrodes, sheath phenomena are responsible for a significant fraction of the total power dissipated by Joule effect, which has detrimental consequences on the electrodes (the cathode in particular), enhancing erosion and reducing its useful lifetime. In particular, a cathode mass loss of 7–23 mg/C is estimated for the ignition procedure used,[17] which gives a tungsten flow contamination of 65–260 ppm at design flow conditions. Flow contamination caused by copper is estimated to be less than 2 ppm. In addition to electrode erosion, some damage to the turbulence enhancing shields was observed. After the initial tests, the shields had to be redesigned to avoid sharp corners, which proved unable to withstand the induced thermal stresses. In any case, no damage was ever observed on the tested models caused by impacting particles; for example, during the shock-wave/boundary-layer interaction test campaign[2] thin-film gauges were used to measure the local heat flux to the model wall without experiencing any damage to the exposed test elements.

Conclusions

Taking advantage of the existing know-how on arcjets and plasma sources for space applications, a pulsed, arc-heated wind tunnel for hypersonic activities has been successfully developed at Centrospazio. Tests carried out so far have shown both the reliability of the arc heater and, in general, the effectiveness of the numerical tools developed for the heater design, despite of their relative simplicity.

More than 600 runs using synthetic air as the working fluid have been performed, with no part replacements and without any significant component damage. As expected, the cathode and ceramic mixing shields proved to be the most stressed and critical components, though operating the facility in a pulsed mode greatly alleviated the problems.[3]

Good repeatability of plenum chamber flow parameters (stagnation pressure and temperature) has been obtained for the operation condition investigated. Furthermore stagnation temperatures in excess of 2500 K have been observed, demonstrating the possibility of extending the arc heater capability beyond the maximum design temperature foreseen at the beginning of the activity.

Acknowledgments

This work was partially financed by ESA under Contract 11.534/95/NL/FG in the framework of the Future European Space Transportation Investigation Program. The authors wish to acknowledge the help of Alessandro Alcamo and Giovanni Pala in setting up the facility. Finally, the tunnel would not have been realized without the support of Mariano Andrenucci and Luca d'Agostino.

References

[1] Scortecci, F., Paganucci, F., d'Agostino, L., and Andrenucci, M., "A New Hypersonic High Enthalpy Wind Tunnel," AIAA Paper 97-3017, July 1997.

[2] Scortecci, F., Paganucci, F., and d'Agostino, L., "Experimental Investigation of Shock-Wave/Boundary-Layer Interactions over an Artificially Heated Model in Hypersonic Flow," AIAA Paper 98-1571, April 1998.

[3] Biagioni, L., Scortecci, F., Paganucci, F., Banetta, S., and d'Agostino, L., "Two Years of Arc-Tunnel Experience at Centrospazio," *Proceedings of the 3rd European Symposium on Aerothermodynamics for Space Vehicles*, ESA, SP-426, Noordwijk, The Netherlands, 1998, pp. 649–657.

[4] Scortecci, F., Paganucci, F., Biagioni, L., Borrelli, S., and Marini, M., "Disegno dell'ugello per una galleria ipersonica ad alta entalpia," *Proceedings XIV Congresso Nazionale AIDAA*, AIDAA, Naples, Italy, 1997, pp. 303–314.

[5] Horn, D. D., Felderman, E. J., and MacDermott, W. N., "Impacts of External Magnetic Fields Applied to High-Pressure Electric Arc Heaters," *Journal of Propulsion and Power*, Vol. 12, No. 6, 1996, pp. 1093–1098.

[6] Blythe, P. A., "Nonequilibrium Flow Through a Nozzle," *Journal of Fluid Mechanics*, Vol. 17, 1963, pp. 126–140.

[7] Wray, K. L., "Chemical Kinetics of High Temperature Air," *Hypersonic Flow Research*, edited by F. R. Riddell, Vol. 7, Progress in Astronautics and Rocketry, Academic, New York, 1962, pp. 181–204.

[8] Landau, L., and Teller, E., "Theory of Sound Dispersion," *Physicaliske Zeitschrift der Sowjetunion*, Vol. 10, No. 1, 1936, pp. 34–43.

[9] Vincenti, W. G., and Kruger, C. H., *Introduction to Physical Gas Dynamics*, Wiley, New York, 1965, pp. 197–244.

[10] Jahn, R. G., *Physics of Electric Propulsion*, McGraw–Hill, New York, 1968, pp. 110–112.

[11] Albertson, C. W., and Bausermann, W. A., "Total Temperature Probes for High-Temperature Hypersonic Boundary-Layer Measurements," NASA TM-4407, March 1993.

[12] Glawe, G. E., Holanda, R., and Krause, L. N., "Recovery and Radiation Corrections and Time Constants of Several Sizes of Screened and Unshielded Thermocouple Probes for Measuring Gas Temperature," NASA TP-1099, Jan. 1978.

[13] Cann, G. L., Buhler, R. D., Harder, R. L., and Moore, R. A., "Basic Research on Gas Flows Through Electric Arcs, Hot Gas Containment Limits," Electro-Optical Systems, Inc., ARL 64-49, Pasadena, CA, March 1964.

[14] Roth, J. R., *Industrial Plasma Engineering—Volume 1*, Inst. of Physics Pub., Bristol, England, UK, 1995, Chap. 10.

[15] Stine, H. A., and Watson, V. R., "The Theoretical Enthalpy Distribution of Air in Steady Flow Along the Axis of a Direct-Current Electric Arc," NASA TN D-1331, Aug. 1962.

[16] Biagioni, L., Scortecci, F., Paganucci, F., d'Agostino, L., and Andrenucci, M., "Performance of Centrospazio Hypersonic High Enthalpy Wind Tunnel," AIAA Paper 98-1508, April 1998.

[17] Auweter-Kurtz, M., Glocker, B., Kurtz, L., Loesener, O., Schrade, H. O., Tubanos, N., Wegmann, T., Willer, D., and Polk, J. E., "Cathode Phenomena in Plasma Thrusters," *Journal of Propulsion and Power*, Vol. 9, No. 6, 1993, pp. 882–888.

M. Torres
Associate Editor